Int. J. Heat Mass Transfer. Vol. 27, No. 6, pp. 901 910, 1984
Printed in Great Britain

0017-9310/84 $3.00 + 0.00

TWO-PHASE DROPLET FLOW CONVECTIVE AND RADIATIVE HEAT TRANSFER

J. N. CHUNG and S. I. OLAFSSON
Department of Mechanical Engineering, Washington State University, Pullman, WA 99164, U.S.A.

(*Received* 7 *January* 1973 *and in revised form* 14 *November* 1983)

Abstract—Numerical solutions of convective and radiative heat transfer to a turbulent two-phase droplet flow in a tube are presented for systems of relatively high pressure and high wall heat flux. The highly nonlinear energy equation of the vapor phase with droplets modeled as heat sinks is solved numerically for the thermal entrance region. Radiation heat transfer among the wall, the vapor and the droplet are included with vapor considered as an optically thick medium. For typical conditions investigated, the effectiveness of the droplets decreases with increasing droplet sizes but the effects of radiation becomes more important for larger droplets. The inclusion of radiation generally lowers the wall temperature by 15%.

NOMENCLATURE

A constant in eddy diffusivity correlation
a_v Rosseland absorption coefficient for vapor
B Spalding number, $[C_p(T-T_s)]/[h_{fg}-q_{rad}/\dot{m}'']$
C_p specific heat of vapor
C_l liquid loading parameter, $\pi N r_0^2 d$
d diameter of droplet
F blackbody factor
f Fanning friction factor
F_1 constant in eddy diffusivity correlation
g acceleration constant due to gravity
h_d droplet heat transfer coefficient
h_x local heat transfer coefficient at the wall
h_{fg} latent heat of vaporization
Ja Jakob number, $[C_p/h_{fg}]\,(q_w r_0/k)$
k thermal conductivity of vapor
K constant in eddy diffusivity correlation
L_m mean beam length
$\dot{m}_l$ mass flow rate of liquid
$\dot{m}''$ mass evaporation rate per unit droplet surface area
$\dot{m}'''_{lv}$ liquid–vapor mass flow rate per unit volume
$\dot{m}_T$ total mass flow rate of mixture
N local number of droplets per unit volume
Nu_d droplet Nusselt number, $(h_d d)/k$
Nu_x local Nusselt number at the wall
Nu_{xs} local equivalent single-phase Nusselt number at the wall
Nu_∞ local equivalent fully developed Nusselt number at the wall
p pressure
Pr Prandtl number of vapor, $(\mu C_p)/k$
Pr_t turbulent Prandtl number, $\varepsilon_M/\varepsilon_H$
q heat flux
r radial coordinate
r_0 tube radius
R nondimensional radial coordinate, r/r_0
Re Reynolds number, $2r_0 u_m/\nu$
Re_d Reynolds number of droplets, $|u_m-u_d|d/\nu$
s heat sink per unit volume
S nondimensional heat sink per unit volume, $(r/q_w)s$
t time
T temperature
u axial vapor velocity
u_d velocity of droplets with respect to the wall
u_m mean velocity of vapor
U nondimensional vapor velocity, $u/2u_m$
X nondimensional axial coordinate, $(x/r_0)/(Re_0\ Pr)$
X_a absorption efficiency
x axial coordinate
Z quality of mixture, $1-\dot{m}_l/\dot{m}_T$.

Greek symbols

β nondimensional turbulent conductivity, k_t/k
Γ drag coefficient ratio, $C_D/C_{D,Stokes}$
γ nondimensional radiative conductivity, k_r/k
ε_M eddy diffusivity of momentum
ε_H eddy diffusivity of heat
θ nondimensional temperature, $[k(T-T_s)]/q_w r_0$
λ wavelength
μ dynamic viscosity of vapor
ν kinematic viscosity of vapor
ρ density
σ Boltzmann's constant
τ optical thickness
τ_A aerodynamic response time.

Subscripts

b bulk mean value
c convective
d droplet
h heating
l liquid
m mean value
0 value at inlet
r radiative
s saturation state
t turbulent
v vapor
w wall.

INTRODUCTION

TWO-PHASE droplet flow exists in many high technology applications. Among these applications are two-phase compact heat exchangers, steam generators, and emergency core cooling systems in nuclear reactors. Proper design relies heavily on the accurate predictions of the transport mechanisms of these systems.

In a two-phase compact heat exchanger, the droplet flow is produced by injection of droplets into a vapor stream to increase the heat transfer coefficient dramatically as the droplets evaporate. While in a steam generator tube, the dispersed flow regime is preceded by a region of annular flow with an evaporating liquid film covering the wall and a core flow of saturated vapor and dispersed droplets. The droplets are formed by shearing off the liquid vapor interface. When the liquid film disappears off the wall, a sharp reduction in the heat transfer coefficient follows and the wall temperature takes a sudden jump (dryout point). The vapor temperature is approximately equal to the saturation temperature in the annular flow regime, but after the dryout point a nonequilibrium state exists and the vapor starts to superheat. The droplets which are at the saturation temperature, will receive heat from the superheated steam, which, in turn, causes them to evaporate and generate saturated steam into the vapor flow. Heat is transferred by convection and radiation from the hot wall to the vapor. The superheated vapor gives off heat to the dispersed phase by convection and radiation.

In addition to this, there are two possible mechanisms whereby heat can be transferred directly from the wall to the dispersed phase. These mechanisms are deposition heat transfer and radiative heat transfer. Deposition heat transfer results when droplets impinge upon the hot wall, absorb heat and evaporate. At very high wall temperatures, the deposition heat transfer becomes very small because the impinging droplets are unable to wet a very hot surface and bounce off the wall, virtually unaffected. If the wall temperature is above the Leidenfrost temperature, a vapor film is formed between the droplet and the wall, reducing the heat transfer drastically. Conversely, the radiative heat transfer shows the opposite trend with wall temperature and becomes increasingly important at an elevated wall temperature.

Dispersed flow heat transfer has received considerable attention in recent years and a number of investigations have been performed, by both experimental and numerical methods. Most of these analyses have been limited to low pressure systems and most have neglected radiation effects because of the relatively low absolute temperatures encountered in these cases.

LITERATURE REVIEW

Sun *et al.* [1] and Andersen and Tien [2] reported the heat transfer for droplet flow in nuclear reactor emergency cooling calculations. These are the only analyses we found in the literature that include a rigorous radiation model in the convective droplet flow. Due to the special geometry of nuclear fuel rod arrangements, they successfully adopted the optically thin approach for the radiation heat transfer. The analytical results compare favorably with experiments.

Koizumi *et al.* [3] reported an experimental investigation and a semi-analytical model for post-dryout heat transfer to R-113. They developed a three path heat transfer model involving heat transfer processes from wall to vapor, from vapor to liquid droplets and from wall to droplets in contact with the wall. Their predictions of wall temperature show good agreement with experimental results for R-113. They concluded that most of the heat transfer is associated with forced convection from wall to vapor stream and that droplets vaporize principally in the superheated vapor flow. The heat transfer to impinging droplets was found to be negligible.

Recently Yao and his co-workers have made pioneering and successful contributions in the development of numerical models for post-dryout droplet flow heat transfer. First, Yao [4] numerically solved the energy equation which includes the axial convection of laminar flow, radial diffusion, and a sink term due to the presence of droplet evaporation. The heat transfer for laminar droplet flow was found to be considerably higher than that of single-phase flow. The effects of droplet size and droplet density on the heat transfer were not presented. Yao and Rane [5] reinvestigated the laminar droplet flow heat transfer and removed the unrealistic assumption of constant droplet size made by Yao [4]. They showed the effects of droplet size variation, vapor velocity increase and droplet density decrease along the tube on the droplet flow heat transfer. Yao and Rane [6] and Rane and Yao [7] also analyzed the turbulent droplet flow problem using the same numerical approach they developed for laminar flow. In their analysis, droplet–wall direct contact heat transfer and thermal radiation exchange were neglected. The droplet size was assumed constant due to low system pressures. Their results compare well with the experimental data of Koizumi *et al.* [3]. Webb and Chen [8] also developed a numerical model for turbulent dispersed flow heat transfer. They also numerically solved the vapor momentum equation.

In many systems of practical interest, the pressure is high, the physical dimensions are large or both. This would invalidate the results of a calculation using the assumption of small optical thickness. It is the purpose of this study to investigate the characteristics of an optically thick system. A system of equations governing the physical behavior will be derived and then solved numerically.

ANALYSIS

The numerical model begins at $x = 0$ which either corresponds to the dryout point in a superheater tube of

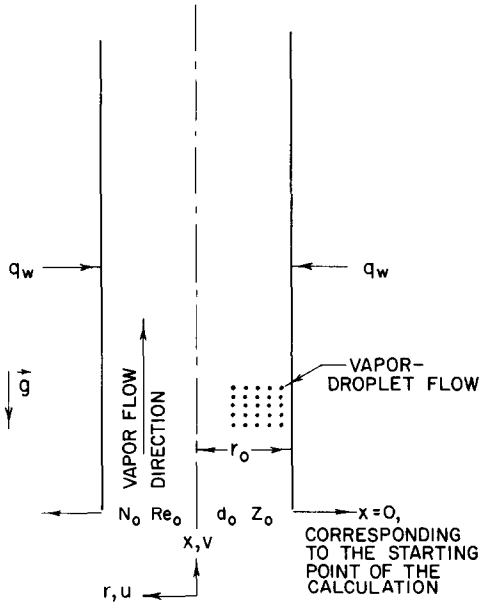

FIG. 1. Schematic diagram of the mathematical model.

a steam generator or represents the point of external injection of droplets into a vapor stream inside a tube of a two-phase compact heat exchanger. The two-phase mixture of initial quality Z_0 and droplet number density N_0 at $x = 0$ is flowing upward inside a vertical circular tube of radius r_0. The schematic of the system is given in Fig. 1.

Assumptions

In the analysis the following major assumptions are made:

(1) The fluid and droplet properties are temperature independent.

(2) The vapor velocity profile is fully developed at the starting point.

(3) The existence of droplets has no effect on the vapor velocity profile and the eddy diffusivity due to relatively high starting quality and small droplets.

(4) The shape of the velocity profile does not change, but the mean velocity, u_m, increases as a result of the evaporation of the droplets.

(5) The droplet distributes uniformly at any cross-section due to turbulent mixing [6].

(6) The droplet diameter is uniform at each cross-section due to radial mixing and uniform evaporation [6].

(7) All droplets diminish in size at the same rate at any axial location [6].

(8) The wall heat flux, q_w, is uniform and constant.

(9) The heat transfer between the droplets and the wall by direct contact is negligible when the temperature of the wall is above the Leidenfrost temperature [9].

(10) The vapor is optically thick due to a relatively large tube size and a high system pressure.

(11) Radiative and conductive heat transfer in the axial direction is negligible due to optically thick vapor and high Peclet number flow.

Governing equations

Based on the above assumptions, the governing equation for the energy transport in the vapor phase may be written as

$$\rho_v C_p u \frac{\partial T}{\partial x} = \frac{1}{r}\frac{\partial}{\partial r}\left((k+k_t+k_r)r\frac{\partial T}{\partial r}\right) - s, \qquad (1)$$

where k is the molecular thermal conductivity, k_t is the turbulent conductivity, and k_r is the radiative conductivity for an optically thick medium and is given by [10]

$$k_r = \frac{16\sigma}{3a_v}T^3. \qquad (2)$$

Here σ is the Boltzmann constant and a_v is the Rosseland absorption coefficient for vapor.

The sink term, s, represents the heat transfer from the vapor phase to the evaporating droplets as a result of the nonequilibrium state in the two-phase mixture where vapor is superheated and droplets stay at the saturation temperature.

The corresponding boundary conditions for equation (1) are

$$(k+k_t+k_r)\frac{\partial T}{\partial r} = q_w - q_{wl} \quad \text{at} \quad r = r_0,$$

$$\frac{\partial T}{\partial r} = 0 \quad \text{at} \quad r = 0, \qquad (3)$$

where q_w is the total heat flux provided by the wall and q_{wl} is the radiative heat flux from the wall to the droplets. The turbulent conductivity is calculated from the two-layer model of Travis *et al.* [11] by assuming a turbulent Prandtl number of 0.9 and

$$k_t = \rho_v C_p \varepsilon_H, \qquad (4)$$

$$\frac{\varepsilon_M}{\nu} = K[y^+ - A\tanh(y^+/A)] \quad \text{for} \quad y^+ < y_i^+, \qquad (5)$$

$$\frac{\varepsilon_M}{\nu} = \frac{K\,Re^+}{12}[1-(F_1R)^2][2/3+2(F_1R)^2]$$

$$\text{for} \quad y^+ \geqslant y_i^+. \qquad (6)$$

In the above, $R = r/r_0$ and y_i^+, F_1, A and K are constants and are given in ref. [11]. Re^+ is the modified Reynolds number of the vapor flow based on the friction velocity, $u_m\sqrt{(f/2)}$

$$Re^+ = Re\sqrt{(f/2)},$$
$$Re = u_m 2r_0/\nu, \quad \tau_w = f\frac{\rho_v u_m^2}{2}, \qquad (7)$$

where τ_w is the wall shear stress, f is the Fanning friction factor, ν is the kinematic viscosity of vapor, and Re is the vapor Reynolds number. The dimensionless variables

are defined in the usual manner

$$y^+ = Re^+(1-R)/2, \qquad u^+ = u/u_m\sqrt{(f/2)}. \tag{8}$$

The three-layer turbulent velocity distributions for fully developed flow presented in ref. [12] are used for velocity profiles of the vapor phase and they are

laminar sublayer:

$$u^+ = y^+, \qquad 0 < y^+ < 5,$$

buffer layer:

$$u^+ = 5 \ln y^+ - 3.05, \qquad 5 \leqslant y^+ < 30,$$

turbulent core:

$$u^+ = 2.5 \ln\left[y^+ \frac{1.5(1+R)}{1+2R^2}\right] + 5.5, \quad y^+ \geqslant 30. \tag{9}$$

The sink term, s, in equation (1) is, in general, a function of r and x and may be expressed as a sum of three contributions, i.e.

$$s = s_c + s_r + s_h. \tag{10}$$

Here s_c is the volumetric convective heat transfer rate from the superheated vapor to the droplets due to relative motion between these two phases, and it may be written as

$$s_c = N\pi d^2 h_d (T - T_s), \tag{11}$$

where N is the droplet number density, d is the droplet diameter, h_d is the convective heat transfer coefficient between the vapor and a single droplet, and T_s is the saturation temperature corresponding to the system pressure. The convective heat transfer coefficient between a vapor and an evaporating droplet can be calculated from a correlation suggested by Yuen and Chen [13]

$$Nu_d = \frac{h_d d}{k} = (2 + 0.6 Re_d^{1/2}\, Pr^{1/3})(1+B), \qquad Re_d = \frac{|u_m - u_d|_d}{\nu}, \tag{12}$$

where u_d is the droplet velocity and Pr is the Prandtl number of the vapor.

The factor $(1+B)$ is introduced for the purpose of correcting the effects of mass transfer due to evaporation on the heat transfer and B, the mass transfer number, is defined as [12]

$$B = C_p(T - T_s) \Big/ \left(h_{fg} - \frac{q_{rad}}{\dot{m}''}\right). \tag{13}$$

Here C_p is the specific heat of vapor, h_{fg} is the latent heat of vaporization based on T_s, q_{rad} is the rate of radiation absorbed by the droplet per unit droplet surface area, and $\dot{m}''$ is the mass evaporation rate per unit droplet surface area. We may write the following for $q_{rad}/\dot{m}''$

$$\frac{q_{rad}}{\dot{m}''} = \frac{2(q_{wl} + q_{vl})}{\dot{m}'''_{lv} r_0}, \tag{14}$$

where $\dot{m}'''_{lv}$ is the mass flow rate of saturated vapor from droplet per unit volume inside the tube, and q_{wl} and q_{vl} are radiative heat transfer rates from the wall to the droplet and from the vapor to the droplets per unit wall area, respectively.

The volumetric radiative heat transfer rate from the vapor to the droplet, s_r, may be written as

$$s_r = \frac{2q_{vl}}{r_0}. \tag{15}$$

We can also express $\dot{m}'''_{lv}$ in terms of heat fluxes and the latent heat of vaporization

$$\dot{m}'''_{lv} = (s_m + 2q_{wl}/r_0)/h_{fg}, \qquad s_m = \frac{2}{r_0^2}\int_0^{r_0} (s_c + s_r) r \, dr. \tag{16}$$

The last term on the RHS of equation (10), s_h, accounts for the sensible heating of raising the temperature of saturated vapor which just flows out of the droplet surface to that of the local superheated vapor

$$s_h = \dot{m}'''_{lv} C_p (T - T_s). \tag{17}$$

Nondimensionalization

The governing equations are nondimensionalized by the following arrangement

$$R = r/r_0, \quad X = (x/r_0)/(Re_0\, Pr), \quad U = u/2u_m, \quad \gamma = k_r/k, \quad \beta = k_l/k, \quad \theta = k(T - T_s)/(q_w r_0), \quad S = (r_0/q_w)s, \quad S_i = (r_0/q_w)s_i, \ \ i = c, r, \text{ or } h, \tag{18}$$

and Re_0 is the vapor phase Reynolds number at $x = 0$.

The dimensionless form of equation (1) is shown as

$$U\frac{\partial\theta}{\partial X} = \frac{1}{R}\frac{\partial}{\partial R}\left((1+B+\gamma)R\frac{\partial\theta}{\partial R}\right) - S. \tag{19}$$

The corresponding boundary conditions are

$$(1+B+\gamma)\frac{\partial\theta}{\partial R} = (1 - q_{wl}/q_w) \quad \text{at} \quad R = 1, \tag{20}$$

$$\frac{\partial\theta}{\partial R} = 0 \quad \text{at} \quad R = 0. \tag{21}$$

The auxilliary equations in dimensionless form are also given below

$$S = S_c + S_r + S_h, \tag{22}$$

$$S_c = Nu_d\, G\theta, \tag{23}$$

where G is the dimensionless liquid loading parameter

$$G = N\pi r_0^2 d, \tag{24}$$

$$S_r = 2q_{vl}/q_w, \tag{25}$$

and

$$S_h = (S_m + 2q_{wl}/q_w)Ja\ \theta, \tag{26}$$

where

$$S_m = 2\int_0^1 (S_c + S_r)R\ \mathrm{d}R, \tag{27}$$

$$Ja = (C_p/h_{fg})(q_w r_0/k). \tag{28}$$

Evaluation of radiative heat fluxes

For a two-phase droplet flow in a circular tube, radiative heat exchanges take place among wall surface, vapor, and droplets. The optical thickness for the vapor phase, τ_v, is estimated, based on the following [1]

$$\tau_v = a_v D, \tag{29}$$

where a_v is the absorption coefficient and D is the tube diameter. For relatively high pressure systems analyzed in this study, the Rosseland mean absorption coefficient can be used for a_v. As shown in the sample calculations, τ_v is $O(1000)$. Therefore, the optically thick assumption is justified for the vapor even when the existence of the droplets is neglected. The presence of the droplets will only increase the optical thickness of the mixture [1]. The radiation heat transfer between the wall and the vapor has been included in the vapor energy equation.

For the liquid phase, we can neglect the scattering because the scattered radiation is predominantly in the forward direction. The absorption coefficient for liquid, a_l, is usually expressed in terms of the geometric cross-section and the number density of the droplets [1]

$$a_l = X_a \pi d^2 N/4. \tag{30}$$

X_a is the absorption efficiency which is found from Mie theory to be [1]

$$X_a = 0.74 \quad \text{if} \quad (\pi d)/\lambda \gg 1, \tag{31}$$

where λ is the wavelength of radiation.

For all the cases in this analysis, $\tau_l = a_l D$ is less than unity. Therefore, we assume that the droplet phase is an optically thin medium. The radiative fluxes from the wall to the vapor and from the vapor to the droplet are now evaluated through the enclosure theory and an equivalent electrical network.

(1) *Vapor to liquid.* The heat flux based on the unit wall area is calculated from

$$q_{vl} = \frac{\sigma(T_m^4 - T_s^4)}{1/\varepsilon_v + 1/\varepsilon_l - 1}, \tag{32}$$

and

$$\varepsilon_v = 1 - \exp(-a_v L_m), \tag{33}$$

$$\varepsilon_l = 1 - \exp(-a_l L_m). \tag{34}$$

The radiant mean vapor temperature, T_m, is defined as

$$T_m = \frac{2}{r_0^2}\int_0^{r_0} Tr\ \mathrm{d}r. \tag{35}$$

L_m is the mean beam length. The value given in ref. [10] for an infinite cylinder and finite optical thickness is adopted for this analysis

$$L_m = 0.95D. \tag{36}$$

(2) *Wall to liquid.* The radiative heat transfer from the wall to the dispersed phase may be found by using the same basic method as above, but some modification has to be included due to the presence of optically thick vapor which absorbs most of the radiation around its absorption bands. A simplified method of estimating the amount of radiation that will reach the droplets through the vapor is developed based on the spectral box model for the absorptivity of the vapor [10]. The absorptivity of the vapor is known to be very dependent upon the wavelength of the radiation. It has a few, very strongly absorbent, bands, but it is practically transparent to radiation in the spectral regions between these bands. The size and the spectral location of the absorbent bands are found by using the exponential wide band model of Edwards and co-workers [10, 14]. The amount of radiative heat transfer is then calculated by assuming that no energy exchange between the wall and droplets takes place in the absorbent bands, but that energy is exchanged freely in the transparent regions between the bands. The heat transfer by radiation in each of the transparent regions is calculated through the blackbody factors and the total heat transfer is the sum of the contributions from each region. The heat flux based on the unit wall area between the wall and the droplets may be written as

$$q_{wl} = \frac{\sigma(F_T(T_w)T_w^4 - F_T(T_s)T_s^4)}{1/\varepsilon_w + 1/\varepsilon_l - 1}, \tag{37}$$

where the wall is assumed to be gray and diffuse and ε_w is the gray emissivity of the wall. The function F_T is defined as

$$F_T(T) = \sum_i (F(\lambda_{iu}, T) - F(\lambda_{il}, T)), \tag{38}$$

where F is the blackbody factor and the index i represents a transparent spectral region in the vapor with an upper and a lower wavelength of λ_{iu} and λ_{il}, respectively.

In the present calculation, the water vapor absorption bands at 6.3, 2.7 and 1.8 μm were used to find the size and the location of the transparent regions.

It should be noted here that the local values of the wall and mean vapor temperatures were used to calculate these radiative heat fluxes. This is a simplification since there could be contributions to these fluxes from upstream and downstream locations, but this simplification is assumed reasonable since the optically dense vapor will quickly absorb radiation

from far away locations and also because the temperatures do not change rapidly in the region of interest.

Droplet motion

The local velocity of the droplets relative to the wall, can be found by solving the following equation of motion

$$\frac{du_d}{dt} = \frac{\Gamma}{\tau_A}(u_m - u_d) - g - \frac{1}{\rho_l}\frac{dP}{dx}, \tag{39}$$

where τ_A, the aerodynamic response time of the droplet, is defined as

$$\tau_A = \frac{\rho_l d^2}{18\mu_v} \tag{40}$$

and Γ is the ratio of the actual drag coefficient to Stokes' drag coefficient. An empirical correlation, valid up to a droplet Reynolds number of 1000 for nonevaporating droplets is [15]

$$\Gamma_0 = 1 + 0.15Re_d^{0.687}. \tag{41}$$

This ratio has to be corrected for an evaporating droplet since the mass transfer tends to decrease the drag coefficient. It becomes

$$\Gamma = \Gamma_0/(1+B), \tag{42}$$

where B is the Spalding number, defined earlier.

The equation of motion can be solved analytically if it is assumed that the droplet diameter and the vapor velocity do not change during the solution interval. The solution is

$$u_d = (u_m - \tau_A F_d/\Gamma)(1 - \exp(-\Gamma t/\tau_A)) + u_{di}\exp(-\Gamma t/\tau_A), \tag{43}$$

where

$$F_d = g + \frac{1}{\rho_l}\frac{dP}{dx}, \tag{44}$$

and u_{di} is the velocity of the droplet at the beginning of the interval. This equation enables a calculation of the droplet velocity at each axial location. The pressure gradient in the vapor can be calculated from

$$\frac{dP}{dx} = -f\frac{\rho_v u_m^2}{r_0}, \tag{45}$$

where f is the Fanning friction factor. The droplet velocity is used to find the local value of the droplet number density from the conservation law

$$N \cdot u_d = \text{const.} \tag{46}$$

The local droplet velocity is also needed in the calculation of the droplet Reynolds number which is used to find the droplet Nusselt number.

The initial droplet number density can be found from the initial mass flow rate of the liquid, $\dot{m}_l$, as follows

$$N_0 = \frac{6\dot{m}_l}{\pi^2 r_0^2 \rho_l d_0^3 u_{d0}}. \tag{47}$$

Change in droplet diameter

The droplet diameter reduction from one axial nodal point to the next can be found from the previously calculated liquid–vapor mass flow rate. The change in mass per unit volume over a length Δx is

$$\Delta M = \frac{\Delta x}{u_d}\dot{m}_{lv}'''. \tag{48}$$

The new droplet diameter becomes

$$d_{j+1} = \left(d_j^3 - \frac{6}{\pi\rho_l}\frac{\Delta x}{u_d}\frac{\dot{m}_{lv}'''}{N}\right)^{1/3}, \tag{49}$$

where N is the local number density of droplets at an axial nodal point j and d_j is the droplet diameter at the jth axial node. This relationship makes it possible to calculate the diameter of the droplets at each axial node as a function of the local conditions and the upstream diameter.

The increase in vapor velocity can also be found from the liquid vapor mass flow rate

$$\Delta u_m = \frac{\dot{m}_{lv}'''\Delta x}{\rho_v}. \tag{50}$$

SOLUTION PROCEDURE

The governing equation, equation (19), subject to boundary conditions, equations (20) and (21), and the auxilliary equations were solved numerically by an implicit finite-difference scheme with cross-stream interaction and marching in the streamwise direction. All the numerical integrations were performed by Simpson's method. The numerical technique is necessary because of the highly nonlinear nature of the governing equation. In the governing equation, γ is a function of the third power of the temperature, S_r is involved with the fourth power of the temperature, and S_h is actually a fifth-order term. The iteration cycle starts with an initial guess or the most recent iterate of temperature to evaluate γ and S. After the procedure of finite differencing, a tridiagonal matrix is formed and it is solved following the procedures in ref. [16]. A variable-spacing grid system was adopted for turbulent flows to increase the accuracy of the solutions. ΔR was in the range 0.00125–0.005 for the near wall region and it was set between 0.025 and 0.05 for the core region. ΔX was found to be appropriate between 5×10^{-6} and 10^{-5}. Both radial and axial step sizes decrease with increasing Re_0 and wall temperatures. All the computations were performed on a Prime 400 computer.

RESULTS AND DISCUSSION

Verification of the computer program

A check of the computer program was performed by comparing the results of wall temperatures with the experimental data for R-113 of Koizumi *et al.* [3]. A favorable agreement was reached as shown in Fig. 2. The experimental study of Koizumi *et al.* [3] is the

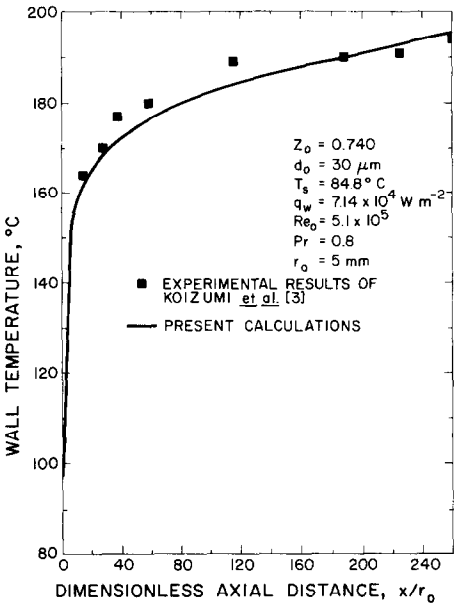

FIG. 2. Comparison with the experimental data of Koizumi *et al.* [3].

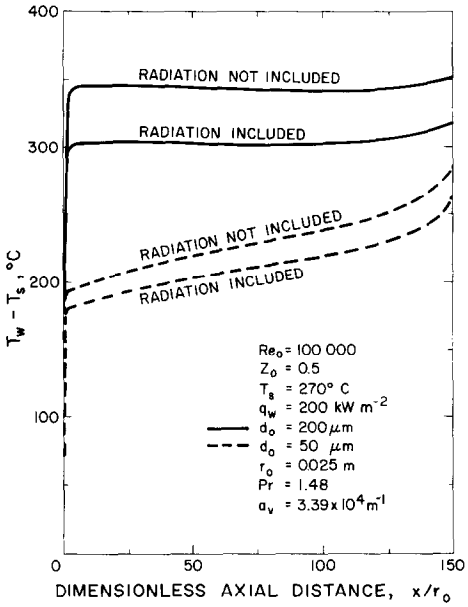

FIG. 4. Comparison of results including radiation vs pure convection for $T_s = 270°C$.

only one known to the authors that reports all the parameters that are needed for a meaningful comparison of this kind. Regrettably, an experimental study cannot be found in the literature that can test the accuracy of the radiation model used here, because of the low absolute temperatures and low system pressures encountered in the experiments.

The effects of radiation

The numerical model was then applied to predict the effect of radiation on the droplet two-phase flow heat transfer under optically thick conditions. At the starting point ($x = 0$), the vapor phase Reynolds number was 100 000 and the quality of the droplet–vapor flow was 0.5. The tube radius was 0.025 m and the constant wall heat flux was 200 kW m^{-2}. Two system saturation temperatures of 200 and 270°C were selected to give optical thicknesses of 478 and 1695 [17] which well qualify the corresponding vapor as an optically thick medium. Initial droplet diameters of 50, 100, and 200 μm were assumed. The comparisons are shown for system saturation temperatures of 200 and 270°C in Figs. 3 and 4, respectively. In general, it is seen that wall temperature is lower for systems with smaller droplets which provides a higher degree of dispersity for a given initial quality. In the case of the smaller droplets (50 μm diameter), the pure convection model is shown to predict wall superheats ($T_w - T_s$) that are about 25% higher than those if radiation is included for a system temperature of 200°C and it is 10% higher for a system temperature of 270°C. For the larger droplets (200 μm diameter), the difference is around 50% for 200°C and 20% for 270°C. The difference between two droplet sizes is explained by the fact that the convective heat transfer from the vapor to the droplets is a stronger function of the degree of dispersity than the radiation heat transfer. Thus, the inclusion of radiation heat transfer becomes more important for larger droplets and a lower saturation temperature.

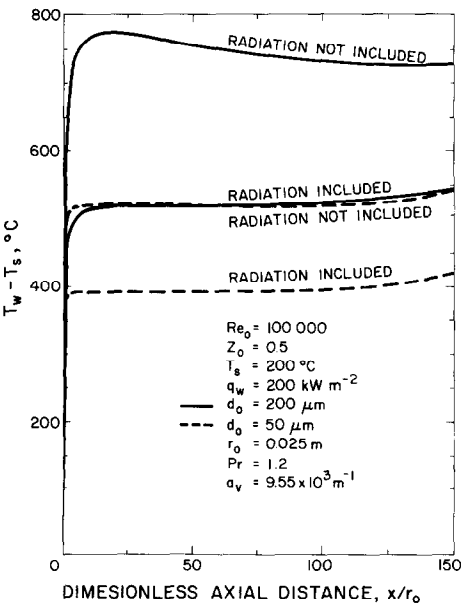

FIG. 3. Comparison of results including radiation vs pure convection for $T_s = 200°C$.

The effects of droplet initial diameter

As explained, the droplet size has a significant effect on the overall transfer mechanism due to the fact that the effectiveness of the convective heat sink can be shown to be inversely proportional to the droplet diameter for equal initial liquid mass flow rates. Figure 5

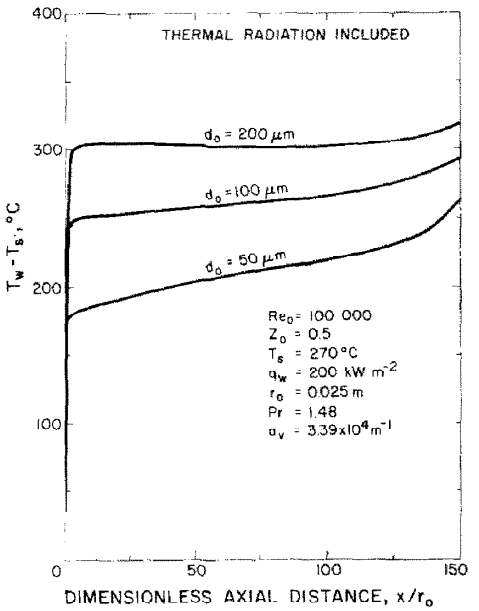

FIG. 5. Variation of wall temperature for three initial droplet diameters.

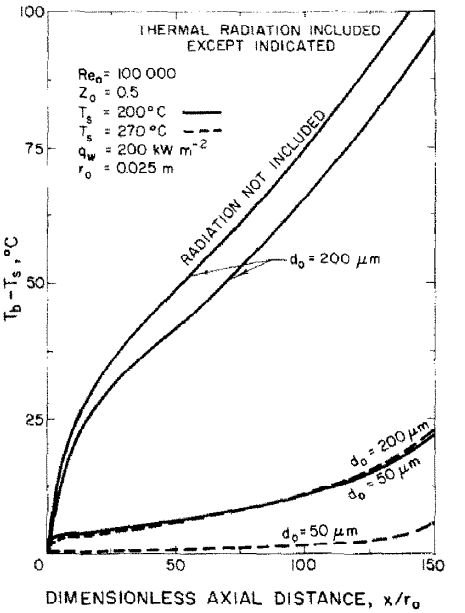

FIG. 6. Variation of bulk mean temperature for two initial droplet diameters.

explicitly demonstrates this trend where the wall temperatures increase with increasing droplet sizes.

With the initial diameters of the droplet as the only varying parameter, three cases of droplet initial diameters varying from 50 to 200 μm were investigated to show some important characteristics of the droplet flow heat transfer. For these cases, the inlet Reynolds number was kept at 100 000, the initial quality was 0.5, the wall heat flux was 200 kW m^{-2}, and the saturation temperature was 270°C.

The bulk mean temperatures

The bulk mean temperature, T_b, of vapor is defined as

$$T_b = \frac{2}{r_0^2 \mu_m} \int_0^{r_0} uTr \, dr. \tag{51}$$

As shown in Fig. 6, the superheat of the bulk mean temperature, $T_b - T_s$, of vapor rises faster for bigger droplets and a lower system saturation temperature. Again this may be explained by the influence of the degree of dispersity on the effectiveness of the heat sink. The radiation effects on the prediction of T_b are significant for an initial droplet diameter of 200 μm and a 200°C saturation temperature case. Only negligible differences were found for the other cases and therefore the comparisons are not shown.

The enhancement of heat transfer due to a dispersed phase

The local two-phase Nusselt number for the current constant wall heat flux case is defined as

$$Nu_x = \frac{2}{\theta_w - \theta_b}, \tag{52}$$

and

$$Nu_x = \frac{h_x 2r_0}{k}, \tag{53}$$

$$q_w = h_x(T_w - T_b), \tag{54}$$

where h_x is the total local heat transfer coefficient. The enhancement of heat transfer due to the presence of dispersed droplets is measured through Nu_x/Nu_{xs}, where Nu_{xs} is the corresponding local Nusselt number for droplet-free, single-phase vapor flow of identical Reynolds number and thermodynamic conditions.

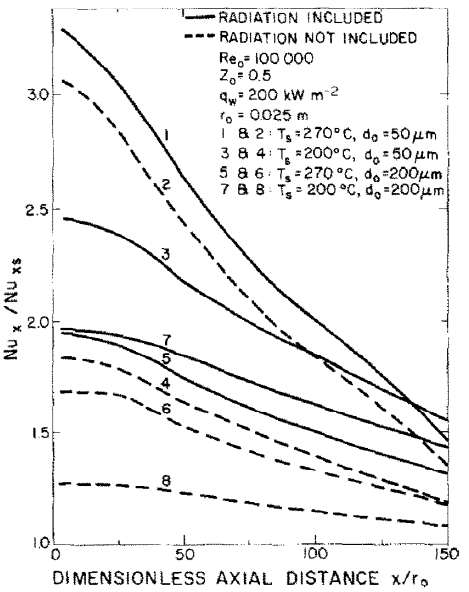

FIG. 7. Nusselt number to local single-phase Nusselt number for two initial droplet diameters.

Since the analysis is in the thermal entrance region, we evaluate Nu_{xs} based on the work of Sparrow *et al.* [18] for Nu_{xs}/Nu_{∞}, where

$$Nu_{\infty} = 0.023 Re_x^{0.8}\, Pr^{0.4}. \quad (55)$$

Re_x is the local vapor-phase Reynolds number and it increases with x due to the evaporation of droplets.

Figure 7 shows the variations of Nu_x/Nu_{xs} as a function of x/r_0. It is indicated by the results that smaller droplets and a higher saturation temperature represent more efficient sink systems. The enhancement decreases with axial distance due to the evaporation of droplets. The numerical model which does not include radiation greatly underestimates the enhancement ratio.

The history of droplet sizes

Figure 8 shows that the change of droplet size is parabolic (D^2-law in two-phase and spray combustion literature). It also indicates that smaller droplets diminish at faster rates. The pure convection model does a better job in predicting the droplet sizes.

Radiative heat fluxes

Figure 9 shows the fraction of radiative heat flux from the wall to the vapor by diffusion to the total wall heat flux, q_{wv}/q_w and the fraction of radiative heat flux from the wall to the droplets to the total wall heat flux, q_{wl}/q_w. We found as high as 30–40% of the wall heat flux is transferred to the vapor by radiation for a system saturation temperature of 200°C. This is consistent with the high wall temperatures shown in Fig. 3. The radiative heat flux from the wall to droplets is also relatively higher for a lower system saturation temperature for the same reason. For a system saturation temperature of 270°C, the radiative heat flux is generally small compared to the convective heat flux.

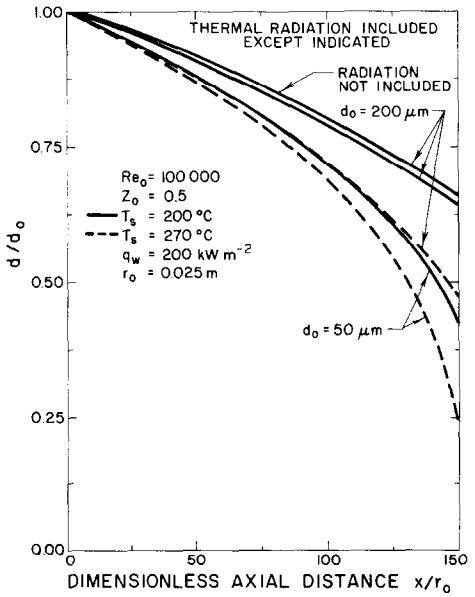

FIG. 8. Droplet size history for two initial droplet sizes.

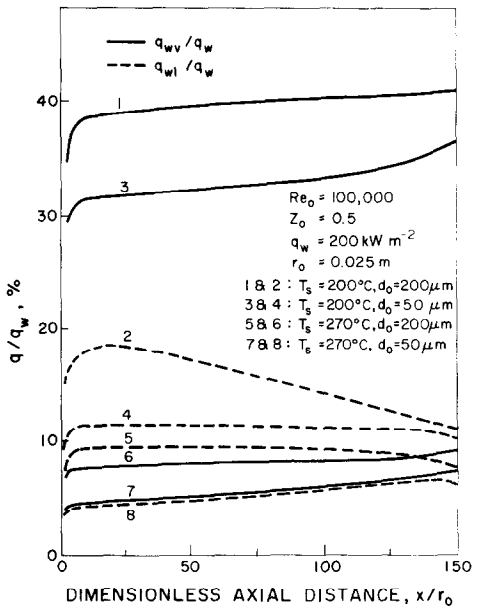

FIG. 9. Ratios of radiative heat flux to total heat flux at the wall for two initial droplet sizes.

CONCLUSIONS

In this paper, a numerical model for predicting the heat transfer mechanism of a two-phase droplet flow was developed. This model extends previous analyses to include the effects of thermal radiation for systems of higher pressures. The results of this study show that the contribution of radiative heat transfer can not be neglected in two-phase systems with moderate to high saturation temperatures and high wall heat fluxes. The radiation heat transfer becomes increasingly important for larger droplets. The sink capacity of the droplets is more efficient for smaller droplets.

Acknowledgements— The authors greatly appreciate the many helpful discussions they had with Professors C. T. Crowe and W. L. Grosshandler. The financial support of the first author from NSF Grant CME-8006762 is gratefully acknowledged.

REFERENCES

1. K. H. Sun, J. M. Gonzalez-Santalo and C. L. Tien, Calculations of combined radiation and convective heat transfer in rod bundles under emergency cooling conditions, *Am. Soc. Mech. Engrs, J. Heat Transfer* **98,** 414–420 (1976).
2. J. G. M. Andersen and C. L. Tien, Radiation heat transfer in a BWR fuel bundle under LOCA conditions, *Fluid Flow and Heat Transfer Over Rod or Tube Bundles*, ASME Symposium Volume, pp. 199–207 (1979).
3. Y. Koizumi, T. Ueda and H. Tanaka, Post-dryout heat transfer to R-113 upward flow in a vertical tube, *Int. J. Heat Mass Transfer* **22,** 669–678 (1979).
4. S. C. Yao, Convective heat transfer of laminar droplet flow in thermal entrance region of circular tubes, *Am. Soc. Mech. Engrs, J. Heat Transfer* **101,** 480–483 (1979).
5. S. C. Yao and A. Rane, Heat transfer of laminar mist flow in tubes, *Am. Soc. Mech. Engrs, J. Heat Transfer* **102,** 678–683 (1980).

6. S. C. Yao and A. Rane, Numerical study of turbulent droplet flow heat transfer, *Int. J. Heat Mass Transfer* **24,** 785–793 (1981).
7. A. G. Rane and S. C. Yao, Convective heat transfer to turbulent droplet flow in circular tubes, *Am. Soc. Mech. Engrs, J. Heat Transfer* **103,** 679–684 (1981).
8. S. W. Webb and J. C. Chen, A numerical model for turbulent non-equilibrium dispersed flow heat transfer, *Int. J. Heat Mass Transfer* **25,** 325–335 (1982).
9. G. E. Kendall, Heat transfer to impacting drops and post critical heat flux dispersed flow, Ph.D. thesis, Massachusetts Institute of Technology, Cambridge, Massachusetts (1978).
10. R. Siegel and J. R. Howell, *Thermal Radiative Heat Transfer* (2nd edn.). Hemisphere, Washington, DC (1981).
11. J. R. Travis, H. O. Buhr and A. Sesonske, A model for velocity and eddy diffusivity distributions in fully turbulent pipe flows, *Can. J. Chem. Engrs* **49,** 14–18 (1971).
12. W. M. Kays and M. E. Crawford, *Convective Heat and Mass Transfer* (2nd edn.). McGraw-Hill, New York (1980).
13. M. C. Yuen and L. W. Chen, Heat-transfer measurements of evaporating liquid droplets, *Int. J. Heat Mass Transfer* **21,** 537–542 (1978).
14. D. K. Edwards and K. E. Nelson, Rapid calculation of radiant energy transfer between nongray walls and isothermal H_2O or CO_2 gas, *Am. Soc. Mech. Engrs, J. Heat Transfer* **84,** 273–278 (1962).
15. R. Clift, J. R. Grace and M. E. Weber, *Bubbles, Drops, and Particles*. Academic Press. New York (1978).
16. S. V. Patankar, *Numerical Heat Transfer and Fluid Flow* (1st edn.), p. 52. Hemisphere, Washington, DC (1980).
17. M. M. Abu-Romia and C. L. Tien, Approximate mean absorption coefficients for infrared radiation of gases, *Am. Soc. Mech. Engrs, J. Heat Transfer* **89,** 321–327 (1967).
18. E. M. Sparrow, T. M. Hallman and R. Siegel, Turbulent heat transfer in the thermal entrance region of a pipe with uniform heat flux, *Appl. Scient. Res.* **7A,** 37–52 (1957).

ECOULEMENT DIPHASIQUE AVEC GOUTTELETTES ET TRANSFERT THERMIQUE PAR CONVECTION ET RAYONNEMENT

Résumé—Des solutions numériques de transfert thermique par convection et rayonnement, pour un écoulement turbulent diphasique avec gouttelettes dans un tube, sont présentées dans le cas de systèmes à relativement haute pression et grand flux pariétal de chaleur. L'équation d'énergie non linéaire de la phase vapeur avec gouttelettes est modélisée avec des sources de chaleur et elle est résolue numériquement pour la région d'entrée. Le transfert radiatif à la paroi, à la vapeur et à la goutte est traité en considérant la vapeur comme un milieu optiquement épais. Pour les conditions typiques étudiées, l'efficacité des gouttelettes décroît quand leur taille augmente mais les effets du rayonnement deviennent plus importants pour des gouttes plus grosses. L'inclusion du rayonnement diminue généralement la température pariétale de 15%.

KONVEKTIVER UND STRAHLUNGS-WÄRMEÜBERGANG BEI EINER ZWEIPHASEN-TROPFEN-STRÖMUNG

Zusammenfassung—Für den konvektiven und den Strahlungs-Wärmeübergang an eine turbulente Zweiphasen-Tropfen-Strömung im Rohr bei relativ hohem Druck und bei hohen Wand-Wärmestromdichten werden numerische Lösungen angegeben. Die stark nicht-lineare Energie-Gleichung der Dampfphase mit den Tropfen als Wärmesenken wird für das thermische Einlaufgebiet numerisch gelöst. Der Strahlungs-Wärmeübergang zwischen Wand, Dampf und Tropfen wird behandelt, wobei der Dampf als 'optisch dickes' Medium betrachtet wird. Für typische untersuchte Zustände nimmt die Wirksamkeit der Tropfen mit wachsender Tropfengrösse ab, wobei jedoch der Einfluss der Strahlung für grössere Tropfen zunimmt. Die Mitberücksichtigung der Strahlung verringert im allgemeinen die Wandtemperatur um 15%.

КОНВЕКТИВНЫЙ И ЛУЧИСТЫЙ ТЕПЛОПЕРЕНОС ПРИ ДВУХФАЗНОМ КАПЕЛЬНОМ ТЕЧЕНИИ

Аннотация—Численно решена задача конвективного и лучистого теплопереноса в турбулентном двухфазном капельном потоке в трубе при относительно высоких давлении и плотности теплового потока на стенке. Нелинейное уравнение энергии для паровой фазы, содержащей капли, которые моделируются как стоки тепла, решено численно для входной тепловой области. Учтен лучистый теплоперенос между стенкой, паром и каплей, причем пар рассматривается как среда с большой оптической толщиной. Для типичных исследованных условий эффективность наличия капель снижается с увеличением их размеров, но для капель большего размера влияние излучения оказывается более существенным. Учет излучения обычно на 15% понижает значение температуры стенки.